A New Method for the Calculation of the Dispersion of Nonperiodic Photonic Crystal Waveguides

Aliakbar Jafarpour, Charles M. Reinke, Ali Adibi, *Senior Member, IEEE*, Yong Xu, and Reginald K. Lee

***Abstract*—We present a new method for the calculation of the dispersion diagrams of general nonuniform waveguides. The method is based on the spatial Fourier transform (SFT) of the electromagnetic field distribution along the guiding direction. We demonstrate the validity and robustness of the SFT technique using several test cases. As an application, we apply the method to analyze the dispersion of biperiodic photonic crystal waveguides and show that the guiding bandwidths of these waveguides can be significantly enhanced by a proper choice of the two distinctive spatial periods of the biperiodic waveguides.**

***Index Terms*—Dispersion, photonic crystal, waveguide.**

I. Introduction

CONVENTIONAL dielectric slab waveguides, which are composed of a slab of dielectric material (core) sandwiched between two layers of other materials (claddings) with smaller permittivity, have become indispensable parts of photonic integrated circuits. Recently, waveguides in photonic crystal (PC) structures have been also extensively investigated [1]–[7]. A PC is a structure with a periodic dielectric constant. Multiple scattering of light from this periodic structure can open a range of frequencies, called photonic bandgap (PBG), with no allowed modes [8]–[12]. A photonic crystal waveguide (PCW) is typically formed by introducing a line defect in a perfect PC. Such conventional PCWs, however, typically cannot achieve guiding over the entire PBG, and may also lead to significant group velocity dispersion (GVD).

Recently, we proposed to use PCWs with two distinctive sets of spatial periodicities to address the problems of a limited guiding bandwidth and a large GVD of the conventional PCWs [13]. This new type of waveguides, which falls under category of quasi-periodic and nonperiodic PCWs, cannot be analyzed using common numerical techniques such as order-N spectral technique [14], plane wave expansion [15], or transfer matrix methods [16], since all these methods depend on the periodicity of the structure in the guiding direction. Using concepts such as "local normal modes" and "coupled modes of an average waveguide," several methods have been developed in the literature for the analysis of nonuniform waveguides [17]–[19]. The method introduced in [19], for instance, expands the guided modes in terms of the "local" uniform waveguide modes, and cannot be readily applied to the analysis of quasi-periodic and nonperiodic PCWs, where it is difficult to define a "local" uniform periodicity.

In this paper, we present an efficient technique for the analysis of dispersion properties of guided modes in nonuniform dielectric waveguides, which is based on the spatial Fourier transform (SFT) of the electromagnetic field distribution of the waveguide modes along the guiding direction. We use the finite difference time domain (FDTD) technique [20] to calculate the field distribution in the waveguide. (In principle, the waveguide field distribution can be calculated by any numerical method for solving Maxwell's equations, and the SFT technique still applies.) Although the method described in this paper is general and can be used for the analysis of any nonuniform waveguide, we apply it to study the properties of biperiodic PCWs, since the guiding performance of these waveguides cannot be easily investigated using the current numerical methods in the literature, as discussed previously.

One intact design parameter in a PCW is the periodicity of the structure in the guiding direction. We recently showed that by changing the periodicity, a more efficient PCW can be designed [13]. We believe that future optimum PCWs will be designed by changing both the size and the periodicity of the air holes next to the guiding region. Thus, an efficient simulation tool, for the analysis of nonperiodic PCWs is urgently needed for the development of photonic crystal circuits. We show that the SFT technique, described in this paper, can be used to find the guided modes of an arbitrary PCW.

The fundamentals of the SFT technique are discussed in Section II, and the method is validated by several tests in Section III. In Section IV, we use the SFT technique to analyze biperiodic PCWs and show how these special waveguides can be used to increase the guiding bandwidth in PCWs. Further details of the numerical implementation of the SFT technique as well as its potential extension are discussed in Section V. Final conclusions are made in Section VI.

II. SFT Technique

Fig. 1(a) shows a small portion of a planar PCW made by removing one row of air holes from a two-dimensional (2-D) triangular lattice of air holes in Si. In general, the periodicity of the air holes next to the guiding region [a' in Fig. 1(a)] can be different from that in the rest of the structure [a in Fig. 1(a)] We begin our analysis by considering the simple case of a PCW with a spatial periodicity of $a' = a$ along the propagation direction. To calculate the mode dispersion diagram of this PCW using the SFT technique, we butt-couple the PCW to a slab waveguide, as shown in Fig. 1(b). For a periodic waveguide, we can classify the PCW mode according to the Bloch wavevector β and

Manuscript received November 20, 2003; revised April 2, 2004.

A. Jafarpour, C. M. Reinke, and A. Adibi are with the School of Electrical and Computer Engineering, Georgia Institute of Technology, Atlanta, 30332 GA USA (e-mail: saman@ece.gatech.edu).

Y. Xu and R. K. Lee are with the Department of Applied Physics, California Institute of Technology, Pasadena, CA 91125 USA.

Digital Object Identifier 10.1109/JQE.2004.831613

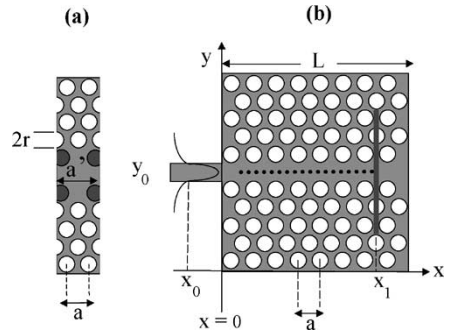

Fig. 1. (a) Biperiodic PCW made by removing one row of air holes from a triangular lattice PC of air holes in Si and introducing a new periodicity (a') in the layers next to the guiding region. Note that $a' = a$ results in a conventional PCW, that is periodic in the guiding direction, x. (b) Basic structure used for the analysis of PCWs with SFT technique. A pulsed Huygen's source is placed in the slab waveguide with thickness h, at $x = x_0$ and the corresponding field is calculated at all points in the dotted horizontal line along the guiding direction (x). For calculation of power transmission spectrum, the Poynting vector is calculated and integrated over a surface at $x = x_1$.

write the field spatial distribution as $\overrightarrow{u}\ (x,y)\exp(i\beta x)$, with $\overrightarrow{u}\ (x,y) = \overrightarrow{u}\ (x+a,y)$. Consequently, the SFT spectrum of this field distribution along the x direction should have peaks located at $\beta + m(2\pi/a)$ (with m being an integer), and we notice that the Bloch wavevector β can be extracted from this SFT analysis without explicitly applying the Bloch theorem.

The concept of Brillouin zone and the Bloch theorem no longer apply to a nonperiodic PCW, which is a nonuniform waveguide. However, it is still possible to express the field in such a waveguide on the basis of a modal expansion at a plane normal to the guiding direction, i.e., $y = y_0$ plane in Fig. 1(b), with, $H_\omega(x,y_0) = \sum_n \hat{H}_{n,\omega} e^{j\beta_{n,\omega}x}$, where $\hat{H}_{n\omega}$ and $\beta_{n,\omega}$ represent the field component and the propagation constant of the n^{th} mode at frequency ω, respectively. Therefore, from, $H_\omega(x,y_0)$, we can extract the peaks of the SFT spectrum, which become well-defined quantities and can be used to describe the propagation of PCW modes if the SFT peaks are independent of both the field components and the choice of y_0.

In order to implement the SFT technique for the calculation of the mode dispersion diagram of a general PCW, we launch a Huygen's source [21] from a slab waveguide toward the PCW and obtain the spatial distribution of one of the six electromagnetic field components (that is not zero everywhere) along the guiding (x) direction, with the y coordinate fixed at y_0 [i.e. $H(x,y_0)$] as shown in Fig. 1(b). All simulations of this paper are performed using the 2-D FDTD technique. In our calculations, we use perfectly matched layer (PML) boundary condition [22] at the four boundaries of the computational domain [see Fig. 1(b)] to simulate the infinite space surrounding the guiding structure and absorb the outgoing radiation.

III. Validation of the SFT Technique

A. Analysis of a Dielectric Slab Waveguide

We have calculated the dispersion diagram of the fundamental transverse magnetic (TM) mode (magnetic field normal to the computation plane; i.e., in the z-direction) of a slab waveguide with Si core and air cladding that is shown in Fig. 2(a). Fig. 2(b) shows this dispersion diagram calculated using the familiar transcendental equation of the slab waveguide [17] and using the SFT technique, with good agreement between the two techniques.

B. Analysis of a Uniform PCW

To establish the validity of the SFT method, we also apply it to analyze the guided modes of a known 2-D PCW, which is constructed by removing one row of air holes in a triangular lattice of air holes in a silicon substrate shown in Fig. 1(a) (with $a' = a$). The lattice period and the air hole radius are represented by a and r, with $r = 0.3a$. Since a large PBG can be obtained for TM polarization (magnetic field parallel to the axes of the air holes) in these PC structures, we limit our discussions to the TM modes of the PCW. The effective Si dielectric constant is chosen to be $\varepsilon_r = 7.9$ to account for the finite thickness of the structure in the normal direction [23]. The PBG for TM polarization in this PC covers the normalized frequency range of $0.253 < a/\lambda < 0.320$ [24], where λ represents the vacuum wavelength. Within the PBG, the PCW supports two TM modes, one with even symmetry and the other one with odd symmetry. In this paper, we concentrate on the fundamental even TM mode, since the odd mode can be pushed out of the PBG by modifying the sizes of the air holes adjacent to the middle slab [24]. We first obtain the dispersion of the PCW by applying the order-N spectral approach [14] to one period of the PCW shown in Fig. 1(a) with Bloch boundary condition applied to the left and right side of the unit cell and the PML boundary condition applied to the top and bottom of the simulation domain. Then, we obtain the waveguide dispersion through the SFT technique as previously described. The dispersion diagrams of both the fundamental and the odd mode of the PCW, obtained from the conventional and the SFT techniques, are shown in Fig. 3. The excellent agreement between the two results demonstrates the validity of the SFT technique.

C. Robustness of the Method

In the SFT technique, the values of the field are calculated along one line in the direction of propagation, i.e., along the $y = y_0$ line in Fig. 1(b). One criterion for reliable extraction of the dispersion relation from the SFT technique is that the resulting dispersion diagrams must be independent of the choice of y_0. Fig. 4(a) shows the dispersion diagrams of the fundamental TM mode of the PCW in Fig. 1(a) (with $a' = a$) for different values of y_0. For simplicity, the center of the PCW has been selected at $y = 0$. Fig. 4 shows that the results of the SFT technique are not affected by the choice of y_0. Although only three cases are shown in Fig. 4(a), we repeated the calculation for several values of y_0. The dispersion diagrams obtained in all cases are practically the same. This shows the robustness of the SFT technique against the choice of y_0. Note that the field amplitude has lateral variations (along the y axis). The fundamental even mode, for instance, has its largest amplitude at the center of the waveguide $(y = 0)$. The larger y_0 is, the smaller the field amplitude at observation points will be. As a result, the signal strength becomes weaker and weaker and eventually comparable to numerical errors at large y_0. Hence, observation points should not be chosen at points with large values of y_0.

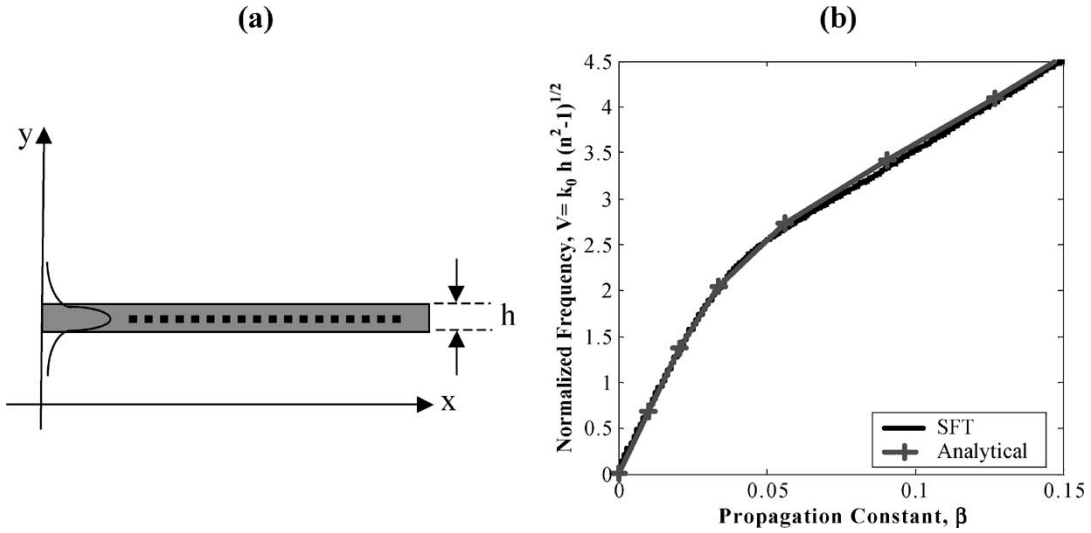

Fig. 2. (a) Slab waveguide with Si core (with thickness h) and air cladding. (b) Dispersion of the fundamental TM mode of the slab waveguide in (a) calculated using the conventional semi-analytical technique and the SFT method. Normalized frequency is denoted by $V = k_0 h\sqrt{n^2-1}$, where k_0 is the free space wavevector, and n is the refractive index of the core.

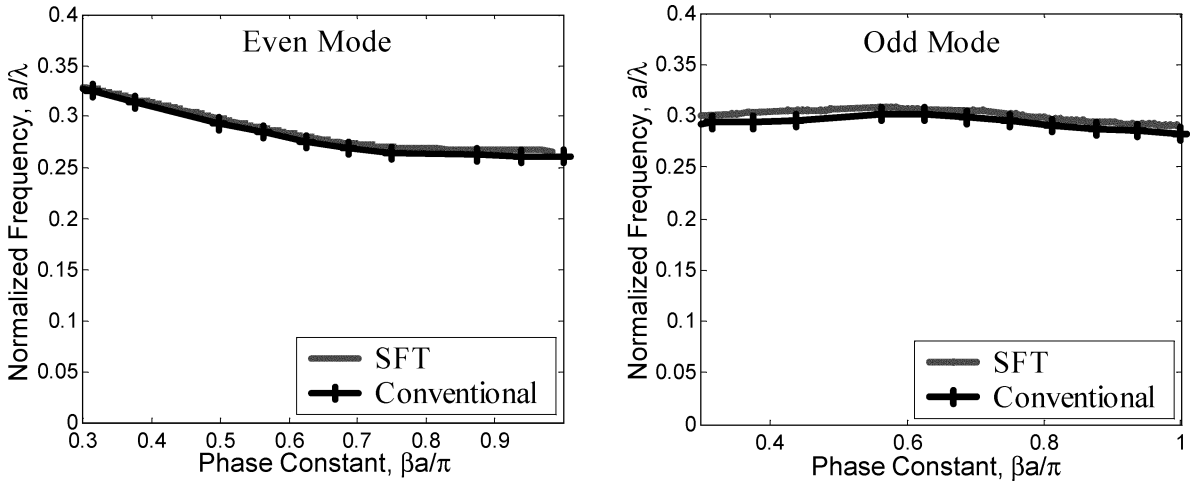

Fig. 3. Dispersion diagrams for the even and odd TM modes of the PCW made by removing one row of air holes from a 2-D PC of holes in Si, calculated using both the conventional (order-N spectral) method and the SFT technique for $r = 0.3a$. The PBG for this PCW covers the normalized frequency range of $0.253 < a/\lambda < 0.320$.

(In general, the observation points must not be selected at points where the field amplitude is close to minimum.)

In the SFT analyses, it is also important to compare the dispersion diagrams for the same mode calculated using different (nonzero) field components. Fig. 4(b) shows the dispersion diagram of the fundamental TM mode of the PCW shown in Fig. 1(a), when different field components are used in the SFT calculations. Since the mode polarization is TM, there are only three nonzero field components, H_z, E_x, and E_y for the coordinate system shown in Fig. 1(b). The results are depicted in Fig. 4(b). It is clear that the dispersion diagram is the same in all cases.

Another important parameter in the SFT technique is the length of the structure (which also defines the maximum number of observation points in the SFT calculations), shown by L in Fig. 1(b). The dispersion diagram of the same PCW, calculated using different values of L, are given in Fig. 5. The lengths have been expressed in units of the lattice constant (a). It is clear from Fig. 5 that all the dispersion diagrams are the same, which is consistent with our expectation that the waveguide dispersion calculated using the SFT technique should be length-independent.

D. Morphology of the SFT Signal

Since we can only consider a finite section of the waveguide in the SFT analysis, the peaks in the numerically obtained SFT spectrum should have finite widths. Fig. 6 shows one SFT calculated using the computation domain in Fig. 1(b) for the PCW described in Section III-C and D at the normalized frequency of $a/\lambda = 0.270$. We have also shown in Fig. 6, the SFT of a simple exponential function $f(x) = e^{j\beta x}$, where β is selected at $\beta = 1.268(\pi/a)$, which coincides with the peak of the SFT of the PCW field at $a/\lambda = 0.270$. The number of samples and the sampling period for the two cases are the same. The full-width–half-maxima (FWHM) are, respectively, $\Delta k_{\text{Field}} =$

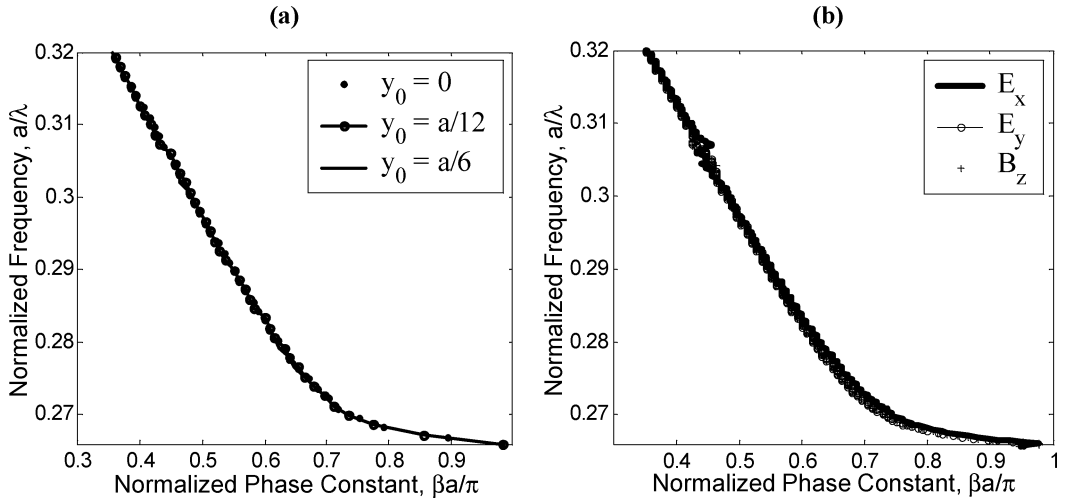

Fig. 4. Effect of (a) the vertical coordinate, y_0, of the observation points, and (b) the field component used in the SFT analysis, on the dispersion diagram of the fundamental TM mode of the PCW shown in Fig. 1(a) with $a' = a$ calculated by the SFT technique. The period of the PCW in the guiding direction is represented by a. Other parameters of the PCW are summarized in the caption of Fig. 3.

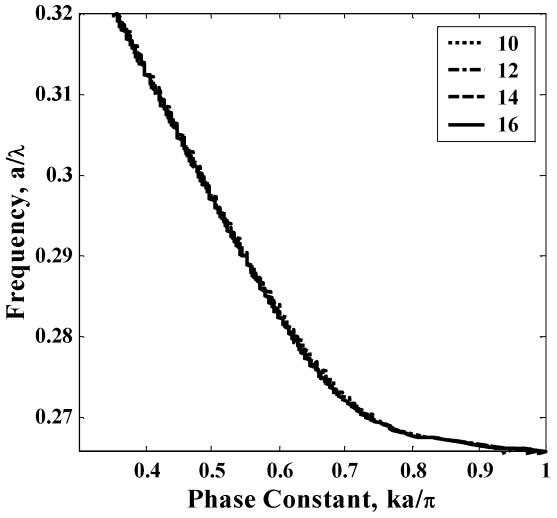

Fig. 5. Effect of the length of the PCW on the dispersion diagram calculated by the SFT technique. Different curves correspond to PCWs with different lengths (L) expressed in units of the lattice constant. The properties of the PCW are the same as those described in the captions of Figs. 3 and 4.

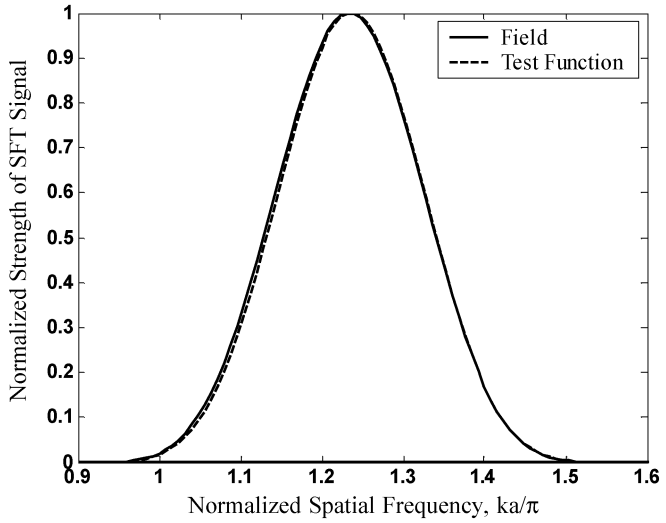

Fig. 6. Normalized strength (magnitude squared) of the SFT of the magnetic field of the fundamental TM mode for the periodic $(a' = a)$ PCW at a frequency of $a/\lambda = 0.270$ and that of a test function $f(x) = e^{j\beta x}$. β corresponds to the peak of the SFT of the field. Both SFTs have sharp peaks corresponding to well-defined modes. The properties of the PCW are the same as those in the captions of Fig. 3.

$0.220(\pi/a)$ and $\Delta k_{\text{Test Sig.}} = 0.211(\pi/a)$. These two numbers are very close to each other, which indicate that the finite width of the SFT spectral peak can be mostly attributed to the finite number of samples used in the Fourier transformation. This comparison, in general, is a useful tool for checking the existence of simple guided modes (expressed by $e^{j\beta x}$ terms) in a nonuniform waveguide.

IV. Applying the SFT Method to Nonperiodic Structures

Up to now, we used different test cases to show the robustness and validity of the SFT technique presented in this paper. However, the main reason for developing this technique is the analysis of nonperiodic PCWs (and in general, nonuniform waveguides) for which the existing techniques of finding guided modes cannot be used to test the existence and to find the dispersion diagram of guided modes (if any). In this section, we apply the SFT technique to the analysis of biperiodic PCWs that are very attractive for increasing the guiding bandwidth of the PCWs. Such a biperiodic PCW can be constructed by choosing different values for a'/a in Fig. 1(a). The primary motivation in designing such structures is to overcome the problem of mode flattening (and thus, limited guiding bandwidth) in a conventional PCW, caused by distributed Bragg reflections (DBR) in the guiding direction [25]. By changing the periodicity of the two rows of air holes that are adjacent to the guiding region, i.e., a', we can move the DBR peak frequency (and thus the mode flattening frequency) out of the PBG [13]. Before analyzing the dispersion diagrams of biperiodic PCWs, it is important to use the SFT analysis to check the existence of the conventional modes that can be

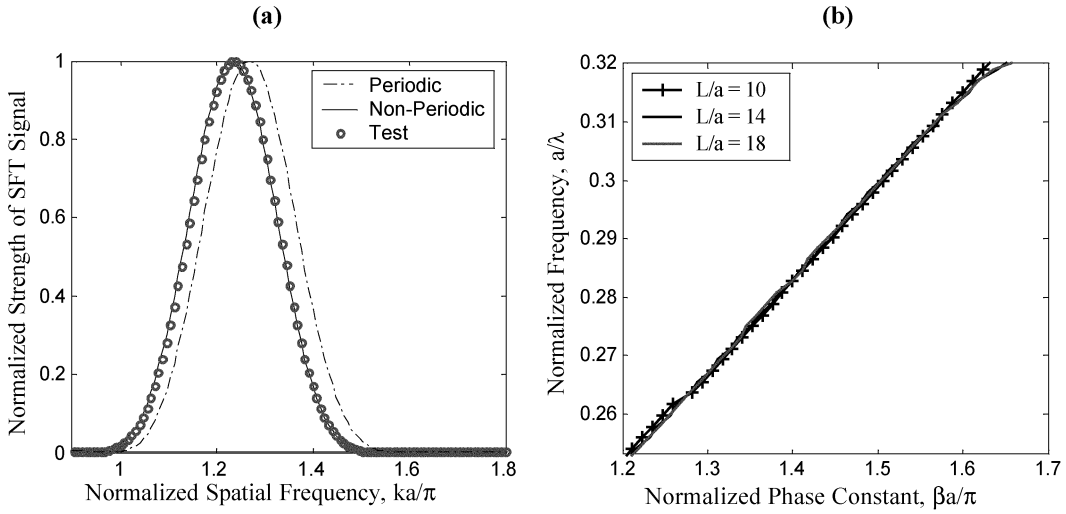

Fig. 7. (a) Normalized strength (magnitude squared) of the SFT of the magnetic field of the fundamental TM mode for the periodic $(a' = a)$ and biperiodic $(a' = 0.7a)$ PCWs at different frequencies and also the SFT of a test function $f(x) = e^{j\beta x}$. (b) Effect of the length of a biperiodic PCW with $a'/a = 0.7$ on the dispersion diagram calculated by the SFT technique. Different curves correspond to PCWs with different lengths (L) expressed in units of the lattice constant. Other properties of the PCWs are the same as those in the captions of Fig. 3.

expressed as $e^{j\beta x}$ terms and carry a net power along the guiding direction.

We first performed a series of SFT simulations covering different values of a'/a and using different normalized frequencies, a/λ. Fig. 7(a) shows a typical SFT spectrum for $a'/a = 0.7$ (the largest deviation from $a'/a = 1$ that we studied) at normalized frequency $a/\lambda = 0.257$. We have also shown the SFT of a single exponential function $f(x) = e^{j\beta x}$, with $\beta = 1.236(\pi/a)$ which corresponds to the peak of the SFT spectrum of the biperiodic PCW at $a/\lambda = 0.257$. The sampling parameters in the two SFT calculations are the same. The existence of a single SFT spectral peak for the PCW and the equality of the widths (and the shapes) of the two SFT spectra in Fig. 7(a) confirm that it is valid to assign a single propagation constant β for these biperiodic PCWs. For the sake of comparison, we have also shown a similar SFT of the periodic $(a'/a = 1)$ PCW in Fig. 7(a) with a peak at a different value of spatial frequency k. The similarity of the shapes of the SFTs of the fields in the periodic and biperiodic PCWs is another indication of the existence of a well-defined propagating mode in these biperiodic PCWs. Also, we point out that in both cases, a single "Flouqet" component carries most of the energy of the guided mode. It justifies truncating the plane wave expansion of the mode at these frequencies and using one component in the forward and one in the backward direction as a good approximation. (Note that we have restricted ourselves to positive spatial frequencies. Similar peaks can be observed at negative values of the spatial frequency.)

After proving the existence of the normal guided modes, we calculated the dispersion diagram of the fundamental mode of the biperiodic PCW with $a'/a = 0.7$ for different waveguide lengths. The results are shown in Fig. 7(b), which also demonstrate the independence of the modal dispersion from the waveguide length. In general, the behavior of a nonuniform waveguide is length-dependent and the resulting $\beta - \omega$ diagram may change as the length of the nonuniform waveguide changes. In other words, different spatial frequencies may be excited in "similar" nonuniform waveguides with different lengths. However, Fig. 7(b) shows that biperiodic PCWs can have the same dispersion over a given range of lengths; a characteristic of a guided mode. We also calculated the dispersion diagram of this fundamental TM mode using different values of y_0 (defined in Fig. 1(b)) and different (nonzero) field components and obtained the same result.

Fig. 8(a) shows the dispersion diagram of the fundamental TM mode of the biperiodic PCW (defined in Fig. 1(a)) with different values of $a' \geq a$. Note that the normalized phase constant $\beta/(\pi/a)$ (dominant spatial frequency) in Fig. 8(a) can be larger than 1, since the dominant "Flouqet" component is not necessarily the zero-order one. The DBR peak frequency (and thus the flattening frequency) moves to lower frequencies as we increase a' [13], [26]. In Fig. 8(a), we notice that for $a' = 1.225a$ the flattening frequency is completely shifted out of the bandgap. As the frequency of the guided mode "enters" into the DBR frequency gap, the modal propagation constant becomes a complex number, whose real part corresponds to the peak of the SFT of the field and the imaginary part accounts for the decaying of the electromagnetic field along the guiding direction. The formation of a frequency bandgap for the guided PCW mode due to the DBR effect can also be clearly seen from the PCW power transmission spectrum.

To calculate the power transmission spectrum, we used a pulsed Huygen's source to excite the fundamental TM mode in the slab waveguide at $x = x_0$ and integrated the Poynting vector over a surface, which is centered at the middle of the PCW and has a width of 2.5 a [as shown in Fig. 1(b)]. The power transmission coefficient was then calculated as the ratio of the transmitted power to the incident power. For more details on the calculation of the power transmission coefficients, the reader should consult [27]. Fig. 8(b) shows the power transmission spectrum calculated at $x_1 = 14a$ [See Fig. 1(b)] for different values of a'/a corresponding to the PCWs analyzed in Fig. 8(a). The broad zero-transmission region in each case is due to the DBR effect. It is clear from Fig. 8(b) that by increasing a'/a, the DBR peak frequency moves to lower

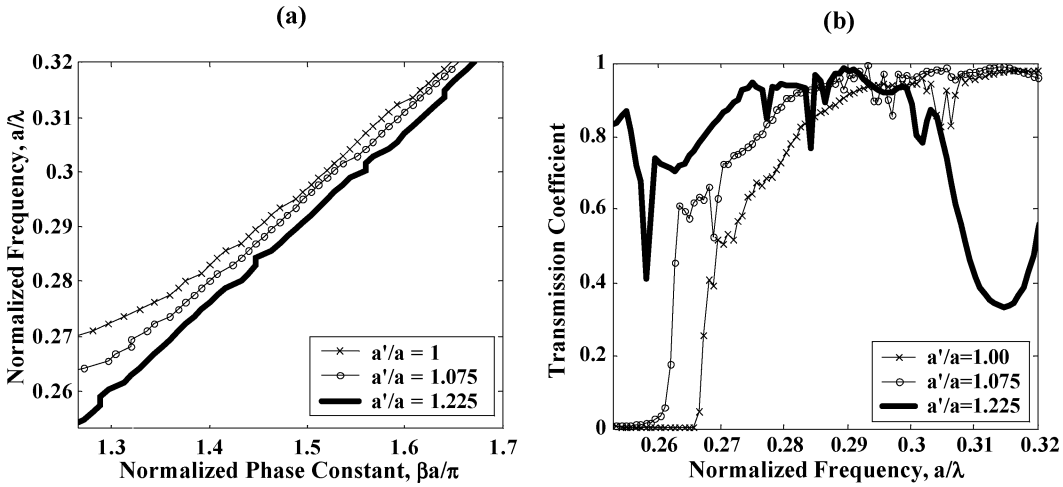

Fig. 8. Evolution of mode flattening and DBR as the periodicity increases. (a) Dispersion diagram of the fundamental TM mode. (b) Power transmission coefficient at $x_1 = 14a$ for the PCW in Fig. 1 with $a' \geq a$. The radius of all air holes is $r = 0.3a$. The normalized frequency range shown in these plots is limited to the PBG of the original photonic crystal.

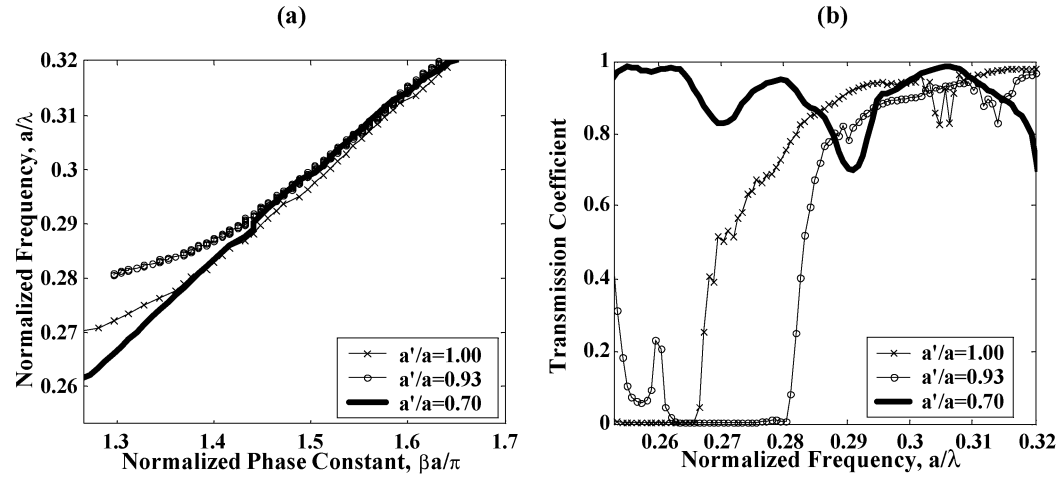

Fig. 9. Evolution of the mode flattening and DBR as the periodicity decreases. (a) Dispersion diagram of the fundamental TM mode. (b) Power transmission coefficient at $x_1 = 14a$ for the PCW in Fig. 1 with $a' \leq a$. The radius of air holes is $r = 0.3a$. The normalized frequency range shown in these plots is limited to the PBG of the original photonic crystal.

frequencies, as expected. For $a' = 1.225a$, the DBR peak (and thus, the mode flattening) frequency is completely out of the PBG and correspondingly the PCW guiding bandwidth covers the entire PBG. We also notice that the flattening frequency for each PCW in Fig. 8(a) coincides with the edge of the transmission minimum in Fig. 8(b).

For the case with $a'/a = 1.225$, we notice that the power transmission of the PCW coupled to a slab waveguide is not optimal in the vicinity of $a/\lambda = 0.26$ and $a/\lambda = 0.31$, even though a guided PCW mode exist in the frequency range under consideration. This illustrates the fact that the existence of a guided PCW mode is a necessary but not sufficient condition for the optical coupling between a slab waveguide and a PCW. In fact, the power transmission from a slab waveguide into a PCW can be severely limited by the impedance mismatch between the slab waveguide mode and the PCW mode, as discussed in [27].

We can also extend the PCW guiding bandwidth by reducing the period of the holes next to the guiding region ($a' \leq a$), which pushes the DBR frequency out of the bandgap. Fig. 9(a) and 9(b) shows the dispersion diagrams of the fundamental guided TM modes and the power transmission spectra, respectively, for three PCWs with different values of $a' \leq a$. Fig. 9 clearly shows that the mode flattening is shifted to higher frequencies (and eventually out of the PBG) by reducing a'/a. For $a' = 0.7a$, the DBR peak frequency and the transmission minimum are shifted completely out of the PBG, increasing the guiding bandwidth to the entire PBG.

The structure with $a' = 0.7a$ seems promising, in the sense of having a linear dispersion diagram going all the way through the bandgap. It also features high transmission at all frequencies within the PBG. Fig. 10 shows the field patterns of this biperiodic PCW (with $a' = 0.7a$) at different frequencies in the bandgap, and clearly demonstrates the efficient coupling and transmission of optical waves within the entire PBG.

V. Discussion

In this paper, we generalize the concept of modal dispersion in a nonuniform waveguide and introduce an intuitive and prac-

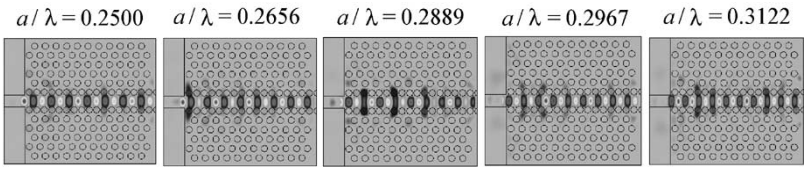

Fig. 10. Field pattern in the PCW with perturbed periodicity of $a' = 0.7a$ at five different frequencies in the PBG. The PBG covers the normalized frequency range of $0.25 \leq a/\lambda \leq 0.32$.

tical method for the investigation of dispersion properties in such waveguides. Once the modal dispersion is obtained, we can test the validity of the results by varying the transverse position, electromagnetic field components, and waveguide length for the nonuniform waveguide under consideration (see Section III-C and D). In the cases of uniform or periodic waveguides, the dispersion diagrams of the waveguide modes obtained using this new approach is the same as those obtained using the more traditional approach (within the precision of our numerical analysis).

Although we focused in this paper on the study of the fundamental guided mode (with even symmetry) of the nonperiodic waveguides, the SFT technique can be used for the analysis of modes with other symmetry properties (for example, odd modes). In analyzing guided modes with a known symmetry, we have to note that the best coupling between a mode of slab waveguide and that of the PCW in Fig. 1(b) is obtained when the beam profiles are the same. So, we use a mode of slab waveguide with a particular parity and order to identify the corresponding mode of the PCW. We particularly consider the first-order even and the first-order odd modes. In practical cases of interest, these are the two possible modes within the PBG (see Fig. 3). We use the first-order even and the first-order odd modes of the slab waveguide for these two cases, respectively. We choose the ordinate of the observation points, i.e., y_0 in Fig. 1(b) so that the field profile is not zero (and preferably is a maximum) at that ordinate. For the first-order even mode, the points are chosen in the middle of the waveguide. For the first-order odd mode, the points have an offset of $\pm h/4$ with respect to the middle of the waveguide, where h is the thickness of the waveguide (We have actually tested both cases of $\pm h/4$ to take numerical errors into account. Both have yielded similar results, as expected).

A propagating mode is neither necessarily guided, nor necessarily real. In other words, a mode may be leaky (couple to the medium surrounding the guide) or it may be complex and carry no net power. As in any other method, we can double-check the results by looking at the field patterns, transmission spectra, and other characteristics of the modes. As a simple criterion, we can fit a negative exponential function on the samples of the field at consecutive points. Relatively large values of the so obtained "attenuation coefficients" can signify complex modes or band edges.

Note that the SFT technique can also be used to find the approximate average modes of even an arbitrary nonuniform waveguide with a specified length. The average modes might be length-dependent depending on the degree of nonuniformity of the waveguiding structure. Again, the relevance of such average modes can be judged by monitoring the width of the SFT peak and comparing it with that of the SFT of a single exponential function as described in Section III-D.

The SFT method outlined in the paper can also find applications in other areas. For example, during the fabrication of any periodic PCW, various lithography steps can introduce certain amount of fabrication imperfections, which can be manifested as variations in the positions and shapes of the air holes in the PCW. Therefore, strictly speaking, the fabricated PCWs are always quasi-periodic. We point out that the method developed in this paper can be used to investigate the impact of fabrication imperfections on the dispersion properties of the actually fabricated PCWs, which is difficult to analyze using other traditional approaches.

VI. Conclusion

We have developed a new numerical method based on the spatial Fourier transformation of the electromagnetic fields for the analysis of the modal dispersion in nonuniform waveguides. We have demonstrated that the SFT approach is both reliable and robust. We have successfully applied this method to study the modal dispersion, field distribution, and transmission properties of the guided mode in a biperiodic PCW. We showed that by changing the periodicity of the PCW in two rows of the air holes that are adjacent to the guiding region, we can increase the guiding bandwidth and obtain PCWs that guide light at all frequencies within the PBG.

References

[1] A. Mekis, J. C. Chen, I. Kurland, S. Fan, P. R. Villeneuve, and J. D. Joannopoulos, "High transmission through sharp bends in photonic crystal waveguides," *Phys. Rev. Lett.*, vol. 77, pp. 3787–3790, 1996.

[2] S. G. Johnson, S. Fan, P. R. Villeneuve, J. D. Joannopoulos, and L. A. Kolodziejski, "Guided modes in photonic crystal slabs," *Phys. Rev. B*, vol. 60, pp. 5751–5758, 1999.

[3] M. Qiu, K. Azizi, A. Karlsson, M. Swillo, and B. Jaskorzynska, "Numerical studies of mode gaps and coupling efficiency for line-defect waveguides in two-dimensional photonic crystals," *Phys. Rev. B*, vol. 64, pp. 155 113–155 117, 2001.

[4] S. Boscolo, C. Conti, M. Midrio, and C. G. Someda, "Numerical analysis of propagation and impedance matching in 2-D photonic crystal waveguides with finite length," *J. Lightwave Technol.*, vol. 20, pp. 304–310, Feb. 2002.

[5] P. Lalanne, "Electromagnetic analysis of photonic crystal waveguides operating above the light cone," *IEEE J. Quantum Electron.*, vol. 38, pp. 800–804, July 2002.

[6] T. Sondergaard, J. Arentoft, and M. Kristensen, "Theoretical analysis of finite-height semiconductor-on-insulator-based planar photonic crystal waveguides," *J. Lightwave Technol*, vol. 20, pp. 1619–1626, Aug. 2002.

[7] E. Lidorikis, M. L. Povinelli, S. G. Johnson, and J. D. Joannopoulos, "Polarization-independent linear waveguides in 3-D photonic crystals," *Phys. Rev. Lett.*, vol. 91, pp. 23 902–23 905, 2003.

[8] E. Yablonovitch, "Inhibited spontaneous emission in solid-state physics and electronics," *Phys. Rev. Lett.*, vol. 58, pp. 2059–2062, 1987.

[9] S. John, "Strong localization of photons in certain disordered dielectric superlattices," *Phys. Rev. Lett.*, vol. 58, pp. 2486–2489, 1987.

[10] K.-M. Ho, C. T. Chan, and C. M. Soukoulis, "Existence of a photonic gap in periodic dielectric structures," *Phys. Rev. Lett.*, vol. 65, pp. 3152–3155, 1990.

[11] W. M. Robertson, G. Arjavalingam, R. D. Meade, K. D. Brommer, A. M. Rappe, and J. D. Joannopoulos, "Measurement of photonic band structure in a two-dimensional periodic dielectric array," *Phys. Rev. Lett.*, vol. 68, pp. 2023–2026, 1992.
[12] K. W. K. Shung and Y. C. Tsai, "Surface effects and band measurements in photonic crystals," *Phys. Rev. B*, vol. 48, pp. 1265–11 269, 1993.
[13] A. Jafarpour, A. Adibi, Y. Xu, and R. K. Lee, "Mode dispersion in biperiodic photonic crystal waveguides," *Phys. Rev. B.*, vol. 68, pp. 233 102–233 105, 2003.
[14] C. T. Chan, Q. L. Yu, and K. M. Ho, "Order-N spectral method for electromagnetic waves," *Phys. Rev. B*, vol. 51, pp. 16 635–16642, 1995.
[15] M. Plihal and A. A. Maradudin, "Photonic band structure of two-dimensional systems: the triangular lattice," *Phys. Rev. B*, vol. 44, pp. 8565–8571, 1991.
[16] B. Gralak, S. Enoch, and G. Tayeb, "From scattering or impedance matrices of gratings to Bloch modes of photonic crystals," *J. Opt. Soc. Amer. A*, vol. 19, pp. 1547–1554, 2002.
[17] D. Marcuse, *Theory of Dielectric Optical Waveguides*, 2nd ed. New York: Academic, 1991.
[18] B. Z. Katsenelenbaum, L. Mercader del Rio, M. Pereyaslavets, M. Sorolla Ayza, and M. Thumm, *Theory of Nonuniform Waveguides: The Cross-Section Method*. London, U.K.: Institute of Electrical Engineers, 1998.
[19] S. G. Johnson, P. Bienstman, M. A. Skorobogatiy, M. Ibanescu, E. Lidorikis, and J. D. Joannopoulos, "Adiabatic theorem and continuous coupled-mode theory for efficient taper transitions in photonic crystals," *Phys. Rev. E*, vol. 66, pp. 66 608–66 622, 2002.
[20] K. S. Yee, "Numerical solution of initial boundary value problems involving Maxwell's equations in isotropic media," *IEEE Trans. Antennas Propag.*, vol. 14, pp. 302–307, May 1966.
[21] D. E. Merewether, R. Fisher, and F. W. Smith, "On implementing a numeric Huygen's source scheme in a finite difference program to illuminate scattering bodies," *IEEE Trans. Nucl. Sci.*, vol. NS-27, pp. 1829–1833, Dec. 1980.
[22] J. P. Berenger, "A perfectly matched layer for the absorption of electromagnetic waves," *J. Comput. Phys.*, vol. 114, pp. 185–200, 1994.
[23] L. A. Coldren and S. W. Corzine, *Diode Lasers and Photonic Integrated Circuits*. New York: Wiley, 1995.
[24] A. Adibi, R. Lee, Y. Xu, A. Yariv, and A. Scherer, "Design of photonic crystal optical waveguides with single mode propagation in the photonic bandgap," *Electron. Lett.*, vol. 16, pp. 1376–1378, 2000.
[25] A. Adibi, Y. Xu, R. K. Lee, M. Loncar, A. Yariv, and A. Scherer, "Role of distributed Bragg reflection in photonic-crystal optical waveguides," *Phys. Rev. B*, vol. 64, pp. 41 102–41 105, 2001.
[26] A. Yariv and P. Yeh, *Optical Waves in Crystals*. New York: Wiley, 1984.
[27] A. Adibi, Y. Xu, R. K. Lee, A. Yariv, and A. Scherer, "Guiding mechanisms in dielectric-core photonic-crystal optical waveguides," *Phys. Rev. B*, vol. 64, pp. 33 308–33 311, 2001.

Aliakbar Jafarpour received the B.Sc. degree in electrical engineering from Shiraz University, Shiraz, Iran, in 1997. He is currently working toward the Ph.D. degree at the Georgia Institute of Technology, Atlanta.

His areas of interests include photonic crystal structures, nonlinear optics, and ultrafast optics.

Charles M. Reinke received the B.S. degree in physics from Jackson State University, Jackson, MS, in 2000 and the B.S.E.E degree from the Georgia Institute of Technology, Atlanta, in 2001, where he is currently working toward the Ph.D. degree in electrical engineering.

His current research projects involve characterization of novel photonic crystal structures as well as studying the effects of nonlinear optical materials in photonic crystals.

Ali Adibi (M'00–SM'04) was born in Shiraz, Iran, in 1967. He received the B.S.E.E. from Shiraz University, Shiraz, in 1990, the M.S.E.E. degree degree from the Georgia Institute of Technology, Atlanta, in 1994, and the Ph.D. degree from the California Institute of Technology, Pasadena, in 1999. His Ph.D. research resulted in a breakthrough in persistent holographic storage in photorefractive crystals.

He worked as a Postdoctoral Scholar at California Institute of Technology from 1999 to 2000. He has been an Assistant Professor in the School of Electrical and Computer Engineering, Georgia Institute of Technology, since 2000. His research interests include holographic data storage, holographic optical elements for optical communications, 3-D optical pattern recognition, design, characterization, and applications of photonic crystals for chip-scale WDM and biosensors, and optical communication and networking. He has been the Conference Chair for the Photonic Bandgap Materials and Devices Conference, Photonic West, since 2001, and the Program Chair for the Nanotechnology program, Photonic West, since 2002.

Dr. Adibi has served as a Technical Committee Member for several conferences including the IEEE Lasers and Electro-Optics Society (LEOS) Annual Meeting. He has also been a Member of the Apker Award Selection Committee since 2002. He is the recipient of numerous awards including the Packard Fellowship (from the David and Lucile Packard Foundation), the National Science Foundation (NSF) Career Award, the Southeastern Center for Electrical Engineering Education (SCEEE) Young Faculty Development Award, the NASA Space Act Award, SPIE's Young Investigator Award, Howard Ector Outstanding Teacher Award from the Georgia Institute of Technology, the Richard M. Bass Outstanding Teacher Award from Georgia Institute of Technology, the Charles H. Wilts Prize for the best electrical engineering thesis of the year from the California Institute of Technology, the New Focus Student Award from the Optical Society of America (OSA), the Top Student (D. J. Lowell) Award from the International Society for Optical Engineering (SPIE), and the Oscar P. Cleaver Award for the Outstanding Electrical Engineering Graduate Student of the Year, from the Georgia Institute of Technology. He is a member of Sigma Xi, OSA, SPIE, and the Materials Information Society (ASM).

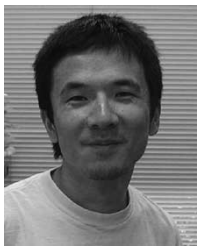

Yong Xu received the B.S. degree in applied physics from Tsinghua University, China, in 1995, and the Ph.D. degree in physics from the California Institute of Technology, Pasadena, in 2001.

His research interests are in the fields of novel photonic structures, fiber optics, nonlinear optics, and laser physics.

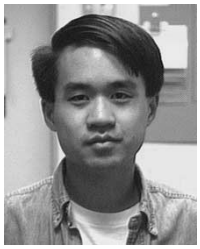

Reginald K. Lee received the B.S degree in aerospace engineering from the University of Toronto, Toronto, ON, Canada, in 1994, and the M.S. and Ph.D. degrees in applied physics from the California Institute of Technology, Pasadena, in 1996 and 2000, respectively.

He is the Director of Product Development at Orbits Lightwave Inc., Pasadena, as well as a Visiting Research Associate at the California Institute of Technology. He has performed some of the first experimental work on active semiconductor photonic crystal structures, among them one of the world's smallest semiconductor lasers.